Robotica (2014) volume 32, pp. 1065–1080. © Cambridge University Press 2014
doi:10.1017/S0263574713001239

Hybrid control for SLIP-based robots running on unknown rough terrain

Bin Han, Xin Luo, Qingyu Liu, Bo Zhou and Xuedong Chen*

State Key Laboratory of Digital Manufacturing Equipment and Technology, Huazhong University of Science and Technology, Wuhan, 430074, People's Republic of China

(Accepted December 7, 2013. First published online: January 15, 2014)

SUMMARY

Rapid and efficient dynamic stability control has been one of the important motivations in legged robot research, especially for legged robots running at high speed and/or on rough terrain. This paper presents a feasible control strategy, named Hybrid Feedback Control (HFC), for running systems based on the spring-loaded inverted pendulum principle (SLIP). The HFC strategy, which comprises two modules (i.e., touchdown angle control and energy compensation), predicts and regulates touchdown angle of the current cycle and need-to-complement energy input of the next cycle through hybrid feedback of flying apex state. This strategy can significantly reduce the computational complexity and enable the system to quickly converge to its control target, meeting the requirements of real-time control. Simulation experiments on various terrains were conducted to verify the adaptability of our HFC strategy. Results of these simulation experiments show that the approach herein can realize the periodical stability control of SLIP systems on different terrain conditions quickly and effectively.

KEYWORDS: Legged robots; Spring-loaded inverted pendulum (SLIP); Hybrid feedback control; Energy compensation; Rough terrain.

1. Introduction

In contrast to wheeled and tracked locomotion, legged locomotion shows promising advantages in traveling speed and rough environment adaption.[1] However, due to the redundancy of multiple legs, joints, and muscles, the legged locomotion exhibits the characteristics of complexity, high–dimension, and non-linearity. Researchers hope to find a simplified model to effectively describe this movement. For animals of different kinds, in spite of their diversity in morphology, they share similarities in aspects of energy metabolism, gait, stride frequency, ground reaction force, etc. Previous research has shown that humans and animals have a system of leg stiffness control. They can change their leg stiffness on demand.[2–5] Through investigation of the ground reaction force pattern, Full[6] found similarities in vertical ground force of two-, four-, six-, and eight-legged in bouncing. His experimental research on locomotion has shown that running animals use multiple legs as a single leg. In two- and four-legged systems, the center of mass (COM) falls to its lowest position at mid-stance just as compressing a virtual leg spring and rebounds during the second half of the step just as recovering stored elastic strain energy. Further, the simple spring-loaded inverted pendulum model (SLIP) is proposed as a template to describe the dynamics of steady legged locomotion over uniform terrain, initially motivated by biomechanical researchers.[7–10] Despite its simple configuration, the SLIP model is very effective to describe dynamic behaviors of animals of many kinds.[11,12] Figure 1 shows that the motion of two- and four-legged creatures can be equivalent to that of a simple SLIP template.

The SLIP model can provide not only a template for biological legged locomotion but also an analytical model for robotic systems because its control laws can be extended to facilitate more

* Corresponding author: E-mail: chenxd@hust.edu.cn

https://doi.org/10.1017/S0263574713001239 Published online by Cambridge University Press

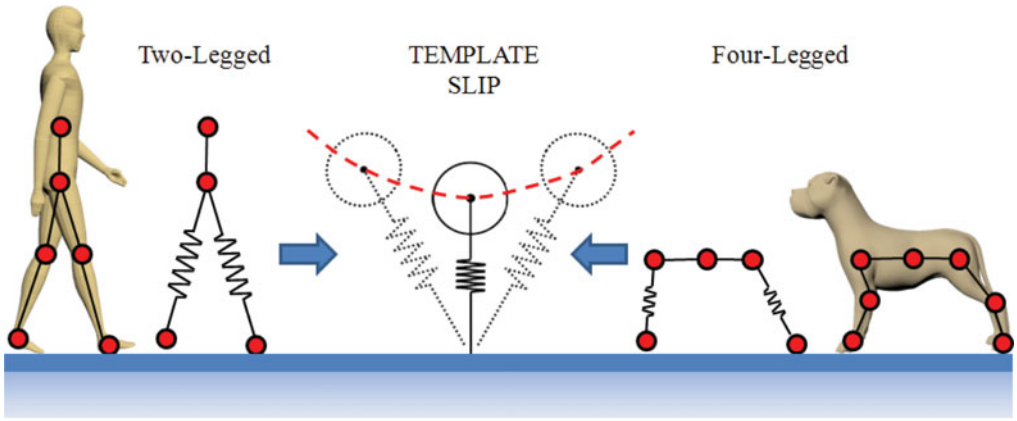

Fig. 1. (Colour online) Motion of two- and four-legged creatures can be equivalent to that of a simple template.

practical leg models.[1,11,13–15] One of the most representative examples employing this idea is a series of hopping machines built by Raibert and his colleagues,[16] and after that, many other hopping robots have been built.[17–21] Nevertheless, how to achieve the periodic steady movement becomes one of the most critical issues for these robots.

Although spring-mass model is quite simple in mechanism, it is not suitable for mathematical analysis, since the model of hopping is a hybrid dynamic system and the dynamic equations in stance are non-integrable due to gravity.[22,23] Fortunately, many researchers have made their efforts to address this issue and some approximate analytical solutions have been proposed extensively in literature.[15,24–26] Most notably, neglecting the damping of the spring, Geyer *et al.* use the Taylor series expansion to obtain an analytical approximation of the SLIP model with gravity considered.[24] This model predicts well the numerical result, which is based on the assumption of a spring angle during stance. An alternative model is presented by Saranli *et al.*[25] In their work an analytic solution is obtained to predict the stance trajectories of a dissipative and torque-actuated planar spring-mass hopper, allowing for a hip torque controller to compensate for damping effects within a stride. These methods can help us find the fixed point of return map under different initial conditions efficiently. However, the methods using approximate solutions to characterize the motion of an SLIP model are sensitive to the initial condition of the system, requiring a large amount of numerical calculations to obtain appropriate initial conditions. We are able to create the return map using these methods, but these are not suitable for the real-time control of an SLIP model.

In the actual system, dynamic real-time control of robots moving on complex terrains has been one of the difficulties in robot control because of the uncertainty of terrain condition and difficulty in contact state modeling. What needed to be considered are real-time control requirements and the environment's influence on system's energy. Fortunately, many scholars have started their research on these ideas. Initially, researchers developed some sophisticated control frameworks based on the assumption that energy in the whole process is preserved.[27,28] However, energy loss exists in reality due to friction, collision, and other factors. From an energy perspective, a walking process of the spring-mass system is a process of energy transformation from the kinetic to the potential, with an additional energy injection to compensate for dissipation. Raibert *et al.*[16] actuated his SLIP hopper with a thrust provided by the hopper's pneumatic mechanism and improved robot's adaptability to multi-terrain locomotion by way of changing its leg length. Zeglin[19] employed compliant leg mechanisms, simplified the control of locomotion on complex terrain, and achieved good robustness. Arslan and Saranli[29] regulated system energy by changing leg length and stiffness, and realized the deadbeat control of hopping machines moving on multi-terrain using three control methods, namely Leg Length Control (LLC), Leg Stiffness Control (LSC), and Two-Phase Stiffness Control (TPSC). This approach has certain adaptability to requirements of different terrain conditions, but requires relatively long-time numerical computation. Schmitt and Clark[30] proposed the active energy removal (AER) control strategy based on active energy addition and removal by leg compression and leg extension. Ahmadi and Buehler[31] presented the controlled passive dynamic running (CPDR) controller imposing desired trajectories via inverse dynamics to reduce energy spent for locomotion. The CPDR strategy

https://doi.org/10.1017/S0263574713001239 Published online by Cambridge University Press

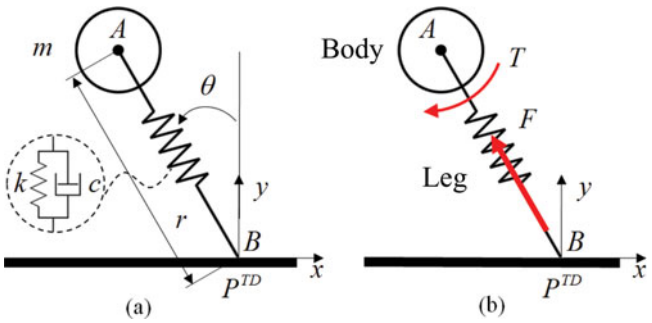

Fig. 2. (Colour online) The SLIP model with damping.

is able to realize the control of hopping height through energy regulation, but the main concerns of this adjustment are robot's vertical velocity components. While these methods have advantages and disadvantages, currently there remains a challenge in the stability control of the SLIP running robots.

The goal of this paper is to propose a simplified strategy based on SLIP model to achieve stable periodic motion. With the application of the proposed strategy, the legged system is aimed to have (i) good real-time performance to meet online requirements, and (ii) better adaptability on uneven terrain. The remainder of this paper is organized as follows. Section 2 describes the equivalent SLIP model with damping in consideration. Section 3 introduces the control structure and details of the Hybrid Feedback Control (HFC) strategy for SLIP stability control. The simulation and results using the HFC method on several different terrains are shown in Section 4. Finally, the concluding remarks and the directions of ongoing work are given in Section 5.

2. Equivalent SLIP Model with Damping

The SLIP model assumes that the equivalent weight load is concentrated on a rigid body, and the leg is massless in order to simplify the complexity of the dynamic computation of the model. Figure 2 illustrates the basic planar SLIP model consisting of a rigid body with mass m attached to a rotating massless leg, where points A and B denote the COM of the body and the foothold point, respectively, and point P^{TD} indicates the location of the model in contact with the ground. The touchdown angle θ is defined as the angle between the spring and the y-axis. As shown in Fig. 2(b), the SLIP model is actuated with two inputs: torque T applied at the hip, and force F acting along the leg. Worth to note is that a multi-joint biological leg with bones and muscles is equivalent to a spring with virtual stiffness k, viscous damping c, and length r between points A and B.

The SLIP model alternates between stance and flight phases during stable running gait as shown in Fig. 3. The flight phase comprises ascent and descent subphases. In this phase the toe loses contact with the ground and the body follows a ballistic trajectory due to gravitational force. The stance phase can be divided into compression and decompression subphases. In this phase the toe remains stationary on the ground with no torque applied at hip.

TOUCHDOWN, BOTTOM, LIFTOFF, and APEX denote four special transition events in the whole running cycle and are defined as the boundaries between descent, compression, decompression, and ascent subphases. For every step, the APEX is triggered when the SLIP reaches its maximum height, where the vertical velocity decreases to zero. Every apex state can be described to characterize the current system, the state variables of which include horizontal velocity $\dot{x}_n$ at the apex, the maximum height y_n^{APEX}, and the total mechanical energy E_n. The apex return map is defined from the current apex variable $U_n[\dot{x}_n, y_n^{\mathrm{APEX}}, E_n]$ to the next apex variable $U_{n+1}[\dot{x}_{n+1}, y_{n+1}^{\mathrm{APEX}}, E_{n+1}]$, where n represents the number of steps counting from 1.

The SLIP model is such a hybrid system that its continuous dynamic change is dependent on the state of ground contact. There are two different dynamic equations in flight phase and stance phase respectively. The flight dynamics of the model in Cartesian coordinates can be easily obtained by

$$\begin{cases} m\ddot{x} = 0 \\ m\ddot{y} = -mg \end{cases}. \tag{1}$$

https://doi.org/10.1017/S0263574713001239 Published online by Cambridge University Press

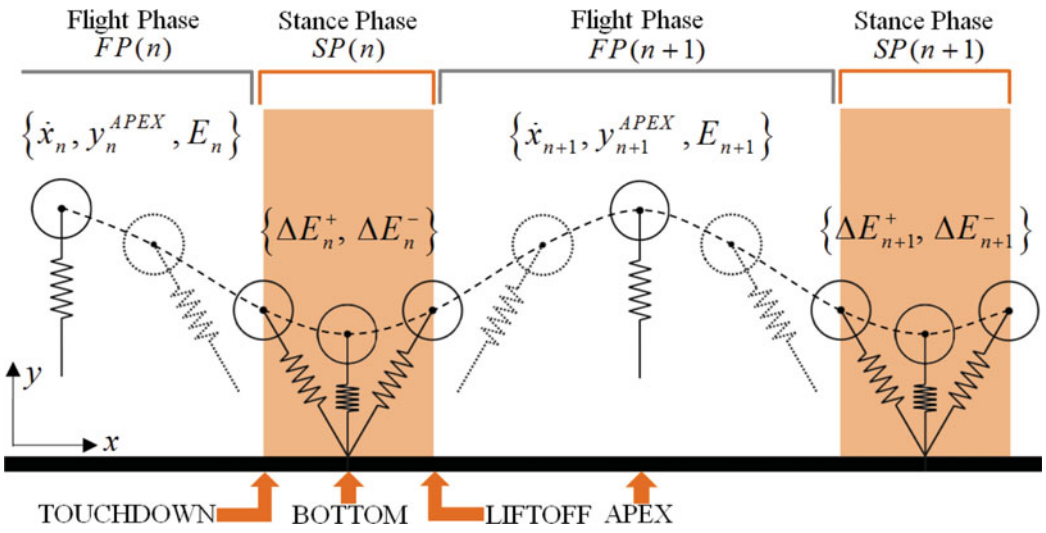

Fig. 3. (Colour online) The SLIP running period, including flight and stance phase with phase transition events.

In the stance phase, the system can be regarded as an inverted pendulum whose hinge is assumed to be fixed on the ground, and can be described using dynamic equation in polar leg coordinates following the Lagrangian method as

$$L = \frac{1}{2}m\dot{r}^2 + \frac{1}{2}mr^2\dot{\theta}^2 - mgr\cos\theta - \frac{1}{2}k\left(r_0^2 - 2r_0r + r^2\right), \tag{2}$$

where r_0 is the leg rest length of the model.

The motion equations of the stance phase can be derived as

$$\begin{cases} m\ddot{r} - m\dot{\theta}^2 r + mg\cos\theta - k(r_0 - r) = -c\dot{r}, \\ 2mr\dot{r}\dot{\theta} + mr^2\ddot{\theta} - mgr\sin\theta = 0. \end{cases} \tag{3}$$

Obviously, Eqs. (3) are coupled nonlinear differential equations, the analytic solution of which does not exist. Several approximations have been proposed under different assumptions, for example, simply linearizing the gravitational force, or assuming small enough relative spring compression rate.[15,24–26] However, we want to find a control method to take into account real-time control requirements and the stability concerns of the periodic motion.

3. Hybrid Feedback Control (HFC)

In spite of the coupling between variables to be controlled, we hope to reduce the complexity of the system's stability control from an overall state point of view. Then a control strategy named HFC is proposed in this paper.

3.1. Control structure for the HFC method

For every SLIP step, the apex state, $U_n[\dot{x}_n, y_n^{\mathrm{APEX}}, E_n]$, can be used to characterize the current system. In order to achieve a stable periodic motion, the goal of the SLIP control system is to make the apex state, $U_n[\dot{x}_n, y_n^{\mathrm{APEX}}, E_n]$, as close as possible to the desired state $U_{\mathrm{des}}[\dot{x}_{\mathrm{des}}, y_{\mathrm{des}}^{\mathrm{APEX}}, E_{\mathrm{des}}]$. The problem for the SLIP control system is to determine the appropriate values of the touchdown angle, θ^{TD}, and the compensational energy, ΔE_n. Therefore, we propose the HFC strategy to solve these problems through a real-time feedback control of the two variables. Figure 4 illustrates the control structure of the HFC strategy.

As shown in Fig. 4, the HFC module consists of two core control modules. One is the touchdown angle control module and the other is the energy compensation control module. At the beginning of the SLIP model's running, a control objective, which can be described by the desired state

https://doi.org/10.1017/S0263574713001239 Published online by Cambridge University Press

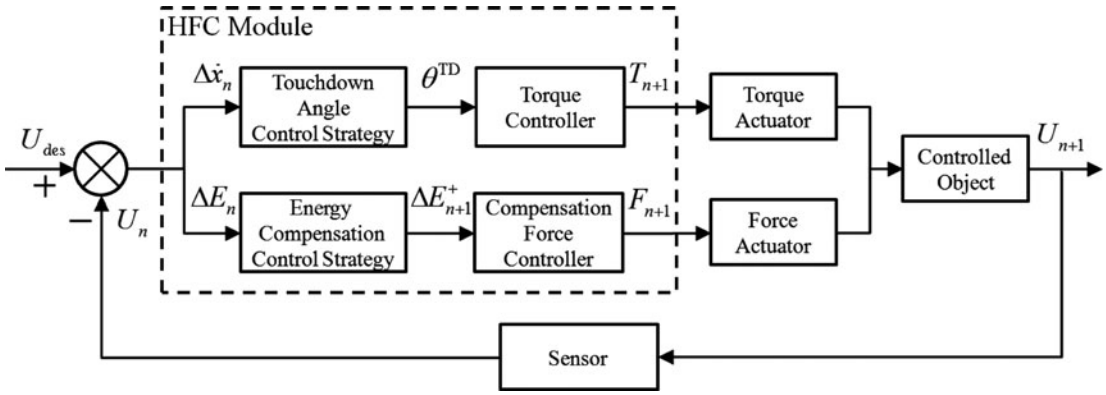

Fig. 4. Control structure schematic of HFC method.

$U_{\text{des}}[\dot{x}_{\text{des}}, y_{\text{des}}^{\text{APEX}}, E_{\text{des}}]$, needs to be set. $\dot{x}_{\text{des}}$ and $y_{\text{des}}^{\text{APEX}}$ represent respectively the desired forward velocity and the desired maximum vertical height at the apex of the SLIP system, and E_{des} denotes the desired total mechanical energy, which can be calculated as follows with variables $\dot{x}_{\text{des}}$ and $y_{\text{des}}^{\text{APEX}}$:

$$E_{\text{des}} = m\dot{x}_{\text{des}}^2/2 + mgy_{\text{des}}^{\text{APEX}}. \tag{4}$$

The current state $U_n[\dot{x}_n, y_n^{\text{APEX}}, E_n]$ can be measured through the sensor module at every apex. Compared with the desired state, we can get the relative velocity error $\Delta\dot{x}_n$ and the relative energy error ΔE_n. Through the touchdown angle control module and the energy compensation control module, the touchdown angle of the next SLIP step, θ^{TD}, and the compensational energy needed in the next stance phase, ΔE_{n+1}^+, can be calculated. After that, the torque, T_{n+1}, and the compensational force, F_{n+1}, for the next SLIP step will be obtained from the PD controller and the compensational force controller. The actuator module guarantees the controlled object to achieve the desired position and complete the next periodic motion. If in every step the apex state is able to reach the desired state $U_{\text{des}}[\dot{x}_{\text{des}}, y_{\text{des}}^{\text{APEX}}, E_{\text{des}}]$ under the control of the HFC module, the SLIP system will run stably and periodically.

3.2. Touchdown angle control strategy

In some previous studies, damping is not considered and the SLIP model is viewed as passive and conservative. For a current state $U_n[\dot{x}_n, y_n^{\text{APEX}}, E_n]$, before touchdown, there is a value of the touchdown angle θ^{TD} at which the system maintains its initial forward speed and apex height after the stance phase. This point where the SLIP model contacts the ground is referred to the neutral point. As Hodgins and Raibert[32] have mentioned, the neutral point corresponds to a symmetric stance phase, where the forward speed and apex heights of lift-off and touchdown are equal. If the SLIP system can be controlled to reach the neutral point in every stride, the model will be able to achieve a stable periodic cycle.

After that, many methods have been proposed in order to effectively get the neutral point.[15,24,25] However, the accurate analytic solution for stance phase remains unsettled. This will result in three different situations between the touchdown point and the neutral point. As shown in Fig. 5, $\dot{x}_n$ and $\dot{x}_{n+1}$ represent the forward speed before and after the stance phase respectively, θ^{TD} is the touchdown angle in this step, and P^{TD} and P^N denote the touchdown point and the neutral point respectively. When the touchdown point coincides the neutral point, the system will keep the original state in the next step (Fig. 5(a), $\dot{x}_n = \dot{x}_{n+1}$). When the touchdown point is perturbed by decreasing the touchdown angle, which means the touchdown angle is smaller than its value at the neutral point, the system will accelerate in the next step (Fig. 5(b), $\dot{x}_n < \dot{x}_{n+1}$). On the other hand, when the touchdown angle is greater than its value at the neutral point, the system will decelerate in the next step (Fig. 5(c), $\dot{x}_n > \dot{x}_{n+1}$).

However, damping must be taken into account in the actual system. In this case, the SLIP model is no longer a conservative system. Even if the system receives energy compensation in the stance phase, it is still difficult to accurately reach the neutral point because of the coupling effects between

https://doi.org/10.1017/S0263574713001239 Published online by Cambridge University Press

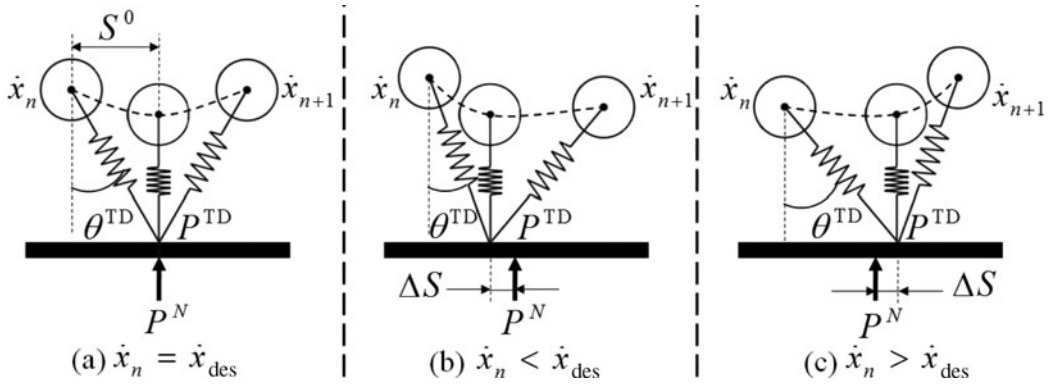

Fig. 5. Three cases of foot placement. (a) Touchdown point coincides with the neutral point. (b) Touchdown point ahead of the neutral point. (c) Touchdown point back of the neutral point.

system's dynamic characteristics. Raibert's foot placement algorithm[16] gives us a viable solution. Therefore, instead of pursuing the exact location of the neutral point, we control the distance between the touchdown point and the neutral point, using it as a feedback. Although there are some error fluctuations, the motion of the SLIP model is able to converge to a stable periodical one within a limited error range. Note that control is based on the previous state as shown in Fig. 3. When the current forward speed $\dot{x}_n$ equals the desired speed $\dot{x}_{\text{des}}$, it can be assumed that the system motion is stable and symmetrical. Besides, during the last stance phase, the touchdown point P^{TD} coincides with the neutral point P^N (Fig. 5(a)). If the current forward speed $\dot{x}_n$ is smaller than the desired speed $\dot{x}_{\text{des}}$, we should set the ground contact point forward the neutral point to create a net forward acceleration (Fig. 5(b)). On the contrary, if the current forward speed $\dot{x}_n$ is greater than the desired speed $\dot{x}_{\text{des}}$, we should set the ground contact point behind the neutral point to create a net rearward acceleration (Fig. 5(c)). Thus, the touchdown angle θ^{TD} can be calculated as follows:

$$\theta_n^{\text{TD}} = \arcsin\left(\left(S_n^0 + \Delta S_n\right)/r_0\right), \tag{5}$$

where S_n^0 is half the distance of the horizontal movement of the COM during the stance phase on the condition that it has achieved symmetry movement, and ΔS_n is the distance between P^{TD} and P^N. The variable S_n^0 can be determined as

$$S_n^0 = \frac{\dot{x}_{n-1}^{\text{avg}} \cdot T_S}{2} = \frac{\left(r_{n-1}^{\text{TD}} \sin\theta_{n-1}^{\text{TD}} - r_{n-1}^{\text{LO}} \sin\theta_{n-1}^{\text{LO}}\right)}{2 \cdot \left(t_{n-1}^{\text{LO}} - t_{n-1}^{\text{TD}}\right)} \cdot \pi\sqrt{\frac{m}{k}}, \tag{6}$$

where $\dot{x}_{n-1}^{\text{avg}}$ is the average forward speed during the stance phase, and T_S is the approximate stance phase time,[21] $(r_{n-1}^{\text{TD}}, \theta_{n-1}^{\text{TD}}, t_{n-1}^{\text{TD}})$ and $(r_{n-1}^{\text{LO}}, \theta_{n-1}^{\text{LO}}, t_{n-1}^{\text{LO}})$ represent the actual leg length, angle and time at touchdown and liftoff phases of the previous stance, respectively. These can be obtained through the sensing system.

As Raibert[16] has mentioned, the control system uses a linear function of the error in forward speed to find a displacement for the foot. Then ΔS_n can be determined as

$$\Delta S_n = \mu \cdot (\dot{x}_n - \dot{x}_{\text{des}}), \tag{7}$$

where μ is the gain selected to maximize stability. Substituting Eqs. (6) and (7) into Eq. (5) yields

$$\theta_n^{\text{TD}} = \arcsin\left(\frac{\pi\left(r_{n-1}^{\text{TD}} \sin\theta_{n-1}^{\text{TD}} - r_{n-1}^{\text{LO}} \sin\theta_{n-1}^{\text{LO}}\right)}{2 \cdot r_0\left(t_{n-1}^{\text{LO}} - t_{n-1}^{\text{TD}}\right)}\sqrt{\frac{m}{k}} + \frac{\mu \cdot (\dot{x}_n - \dot{x}_{\text{des}})}{r_0}\right). \tag{8}$$

https://doi.org/10.1017/S0263574713001239 Published online by Cambridge University Press

3.3. Energy compensation strategy

In order to reduce the complexity of the SLIP model, most existing works completely ignore the effect of damping.[14,24] However, in the practical system, a variety of energy consumption ways are essential, such as drive damping, joint friction damping, foot–ground impact, and so on. We cannot ignore the damping anymore and should make up for the system energy as accurately as possible for physical robot platforms. Some studies have also considered energy compensation,[16] but the common method is to add a fixed amount of energy into the system which may be able to meet the requirements of SLIP model's steady running on a flat terrain. However, this approach may not work well when the terrain is uneven. In this paper we attempt to propose a feasible method for energy compensation even on an uneven ground.

The energy loss can be estimated for the SLIP system on a flat ground.[18,33] When the ground is uneven, the amount of energy loss is no longer easy to calculate accurately. In the HFC method, we use feedback regulation instead of accurate calculation of the energy loss, and the SLIP model will gradually converge to the control target within limited steps. As shown in Fig. 3, energy assessment involves two successive strides with Step(n) and Step(n+1), for example. When the system state converges to the steady state, the fluctuation of the energy loss gets smaller. Therefore, we assume that the energy loss of the system to be the same as the previous one. In the Step(n), ΔE_n^+ and ΔE_n^- denote the amount of energy added and lost during the stance phase respectively. After the liftoff event, the amount of energy loss ΔE_n^- can be calculated as follows:

$$\Delta E_n^- = E_n^{\mathrm{TD}} + \Delta E_n^+ - E_n^{\mathrm{LO}}, \tag{9}$$

where E_n^{TD} and E_n^{LO} denote the total mechanical energy at touchdown event and liftoff event respectively. The current total system energy consists of the kinetic energy, the gravitational potential energy relative to the ground and the elastic potential energy of the spring. E_n^{TD} and E_n^{LO} can be determined as follows:

$$\begin{aligned} E_n^{\mathrm{TD}} &= m\left(\left(\dot{x}_n^{\mathrm{TD}}\right)^2 + \left(\dot{y}_n^{\mathrm{TD}}\right)^2\right)/2 + mgr_n^{\mathrm{TD}}\cos\theta_n^{\mathrm{TD}} + k\left(r_n^{\mathrm{TD}} - r_0\right)^2/2, \\ E_n^{\mathrm{LO}} &= m\left((\dot{x}_n^{\mathrm{LO}})^2 + \left(\dot{y}_n^{\mathrm{LO}}\right)^2\right)/2 + mgr_n^{\mathrm{LO}}\cos\theta_n^{\mathrm{LO}} + k\left(r_n^{\mathrm{LO}} - r_0\right)^2/2, \end{aligned} \tag{10}$$

where $(\dot{x}_n^{\mathrm{TD}}, \dot{y}_n^{\mathrm{TD}}, r_n^{\mathrm{TD}}, \theta_n^{\mathrm{TD}})$ and $(\dot{x}_n^{\mathrm{LO}}, \dot{y}_n^{\mathrm{LO}}, r_n^{\mathrm{LO}}, \theta_n^{\mathrm{LO}})$ represent horizontal velocity, vertical velocity, leg length, and angle at touchdown and liftoff events of the Step(n) respectively. Since the system is energy-conservative in the flight phase, the total energy of the flight phase of Step(n) and Step(n+1) can be described with E_n^{TD} and E_n^{LO} respectively, or be characterized by the vertical height and horizontal velocity of the apex on a flat terrain. Nevertheless, Eq. (9) takes into account terrain changes. Difference in foothold height alters the potential energy of the system, so in spite of terrain changes, the variation in the system energy can be obtained easily. Besides, this method needs no additional sensor to detect apex height. Basic velocity sensor and leg length sensor would be sufficient.

Before the next touchdown event, the amount of compensational energy needs to be estimated in advance. The HFC method not only considers the energy error between the current and desired states but also provides an additional value, which may be lost during the next stance phase. Note that the additional energy is consistent with the energy loss during the previous step. The amount of compensational energy in the Step(n+1) can be calculated as follows:

$$\Delta E_{n+1}^+ = E_{\mathrm{des}} + \Delta E_n^- - E_n^{\mathrm{LO}}. \tag{11}$$

The value of stride number n starts from one, and the initial value of ΔE_n^+ is set to zero. The HFC method employs feedback regulation and finally achieves a stable energy control for the SLIP system.

3.4. Optimal choice of the compensational force

In a practical system, actuators provide compensational force to meet the demand of energy supplement. We compare three control strategies for compensational force and try to find an optimal

https://doi.org/10.1017/S0263574713001239 Published online by Cambridge University Press

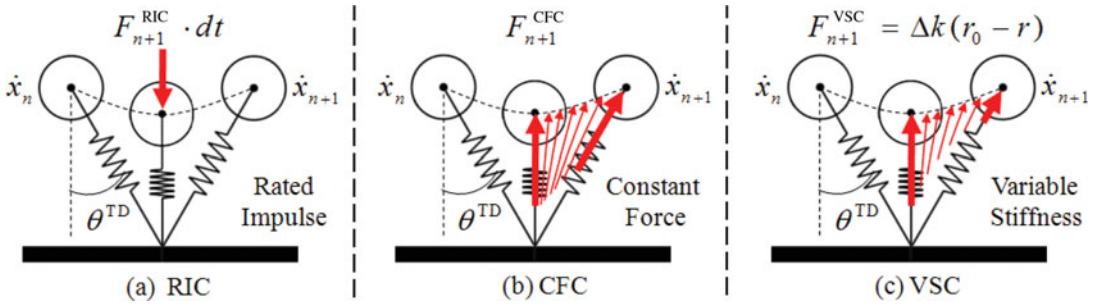

Fig. 6. (Colour online) Three different control strategies for compensation force. (a) Rated Impulse Control (RIC). (b) Constant Force Control (CFC). (c) Variable Stiffness Control (VSC).

choice in this paper. These strategies are Rated Impulse Control (RIC; Fig. 6(a)), Constant Force Control (CFC; Fig. 6(b)) and Variable Stiffness Control (VSC; Fig. 6(c)).

The RIC method compensates for the energy loss by providing an impulse along the spring direction of the system in each stride by actuators. The impulse begins at the time of the maximum leg compression with the vertical velocity of the system being zero at this moment. In this case, the compensational force F_{n+1} can be calculated based on the theorem of impulse as

$$F_{n+1}^{\mathrm{RIC}} = \frac{\sqrt{2m \cdot \Delta E_{n+1}^{+}}}{dt}, \tag{12}$$

where dt is the impulse acting time, and the smaller the dt, the more accurate is our result of energy compensation.

The CFC method provides for the SLIP system a constant force along the spring direction for energy compensation. This constant force acts during the decompression subphase from the bottom event to the liftoff event. Similarly, the compensation force F_{n+1} can be determined as

$$F_{n+1}^{\mathrm{CFC}} = \frac{\Delta E_{n+1}^{+}}{r_0 - r_B}, \tag{13}$$

where r_B represents the leg length at bottom.

The VSC method adjusts the total mechanical energy by controlling leg stiffness during the stance phase. Inspired by the leg stiffness control system of humans and animals, the decompression leg stiffness must be greater in order to increase the total system energy. Extra stiffness Δk is increased in the decompression subphase and can be determined as

$$\Delta k = \frac{2 \cdot \Delta E_{n+1}^{+}}{(r_0 - r_B)^2}. \tag{14}$$

Thus, the compensational force F_{n+1} can be calculated based on the Hooke's Law as follows:

$$F_{n+1}^{\mathrm{VSC}} = \Delta k \cdot (r_0 - r) = \frac{2 \cdot \Delta E_{n+1}^{+} \cdot (r_0 - r)}{(r_0 - r_B)^2}. \tag{15}$$

The above-mentioned methods can realize energy compensation for the SLIP system. However, there are advantages and disadvantages of these methods. For instance, the RIC method requires small enough acting time in order to obtain accurate energy compensation values. This is entirely feasible in the simulation system, but is impractical in the actual system due to the response speed of actuators. For the CFC method, the constant force can be set during the decompression subphase, nevertheless, it's not reasonable that actuators still continue to provide a constant force before the liftoff event. In comparison, the VSC method is more consistent with the biological regulation mechanism of

https://doi.org/10.1017/S0263574713001239 Published online by Cambridge University Press

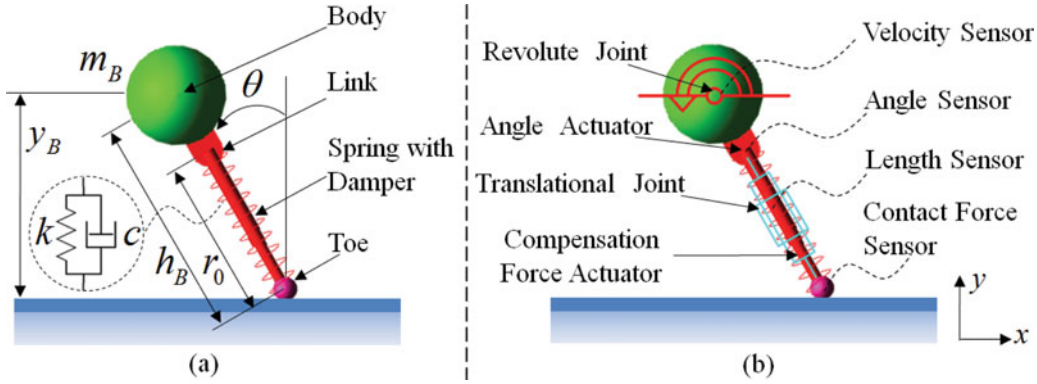

Fig. 7. (Colour online) Simulation model of the SLIP running system in ADAMS.

leg stiffness, and it is achievable in physical robot platforms. Therefore, we choose to use the VSC method for energy compensation in the HFC method.

4. Simulation and Results

In order to verify the correctness and effectiveness of the HFC method, we design the dynamic model of the SLIP system on different terrains using ADAMS, which is a virtual prototype analysis software belonging to MSC Software Corporation, and establish the HFC control model using MATLAB/Simulink. With the co-simulation technique, we test the real-time stability control for the SLIP model in a variety of circumstances, such as inplace vertical jumping, running on the flat terrain, running on the sunken terrain, running down the stairs, and so on. The communication interval between ADAMS and Simulink is 0.0001 sec for all simulations.

4.1. Simulation modeling

An SLIP running model is established in ADAMS environment. Figure 7 illustrates the detailed structure and sensor system of the model. Our SLIP system consists of a body, a link, a spring with damper and a toe (Fig. 7(a)). We regard the equivalent mass of the system to be loaded concentrated on body COM. The link plays the role of a connector between the body and the spring. In the SLIP template, there is nothing at the end of the spring and the spring is directly in contact with the ground. However, a toe is fixed at the end of the spring in our model to facilitate the CONTACT setting in ADAMS environment. Simulation model should best reflect the actual system, therefore the sensor and actuator systems are added into the SLIP simulation model. The velocity sensor is set at the body COM and used to detect the vertical and forward speed of the body COM.

Angle sensor is set on the link, used to obtain swinging angle of the leg. Leg-length sensor, put on the spring, can detect the real-time change of the leg length in the process of movement. Contact sensor on the toe measures the contact force between the SLIP system and the ground, and decides accordingly whether the system has touched or left the ground.

A revolute joint is set between the body and the link, and another translational joint is set between the link and the toe along the spring. In addition, active controlled actuators include angle actuator and compensational force actuator, which are set respectively on the link and equivalent spring, realizing the stability of the system through the outputs of the controlling torque T and the compensational force F (Fig. 7(b)). The established SLIP model takes physiological index of physical dogs as indicated in Table I.

The equivalent stiffness of an SLIP model can be regarded as that of two parallel legs. Then the stiffness of the spring is set to 6 kN/m according to the requirements of equivalent stiffness. Although link and toe in our model are massless in principle, we set their negligible mass for dynamic simulation requirements. Physical parameters of the model are shown in Table II. The initial conditions of simulation experiments include the initial horizontal velocity and the apex height. In literature we refer to the running speed of the dog as 2.8 m/s,[35] with the apex height information not mentioned. Considering that our proposed method is not sensitive to the initial conditions, we

https://doi.org/10.1017/S0263574713001239 Published online by Cambridge University Press

Table I. Physiological index of physical dogs[34,35].

Description	Value
Body mass	23.6 kg
Average leg length	0.5 m
Running speed	2.8 m/s
Front leg stiffness	2.9 kN/m
Rear leg stiffness	1.9 kN/m

Table II. Physical parameters of SLIP model.

Parameter	Description	Value
m_B	Mass of the body	23.6 kg
m_{Link}	Mass of the link	0.005 kg
m_{Toe}	Mass of the toe	0.003 kg
h_B	Distance between toe and COM	0.7 m
r_0	Nominal spring length	0.5 m
k	Spring stiffness	6 kN/m
c	Spring damping	0.01 kN/m
μ	Gain constant	0.1

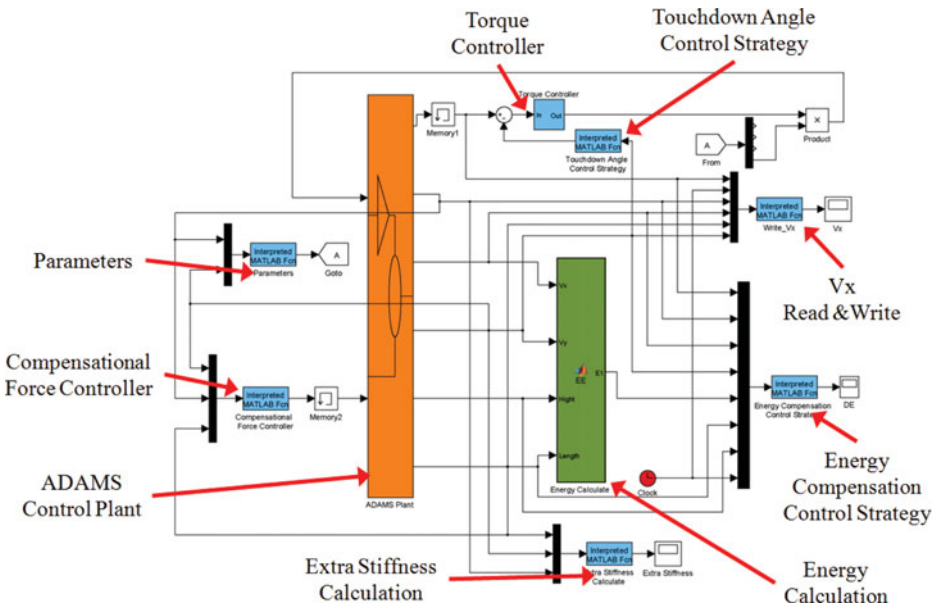

Fig. 8. (Colour online) Co-simulation model in MATLAB/Simulink.

estimate the distance between the toe and the ground in flight phase as about 100 mm for a running dog. Adding the distance between the toe and COM (700 mm) and the toe radius (40 mm), the apex height can be estimated to be 840 mm.

After modeling in ADAMS, we generate the ADAMS control plant and import it into Matlab/Simulink. Then we convert the HFC strategy into Matlab and design the co-simulation model in MATLAB/Simulink. Figure 8 shows the co-simulation model for the SLIP running simulation experiments in this paper.

4.2. Inplace vertical jumping

In order to verify our HFC strategy, first an inplace vertical jumping simulation experiment is designed. The initial height of the apex is set to a constant value of 840 mm, while both initial and expected

https://doi.org/10.1017/S0263574713001239 Published online by Cambridge University Press

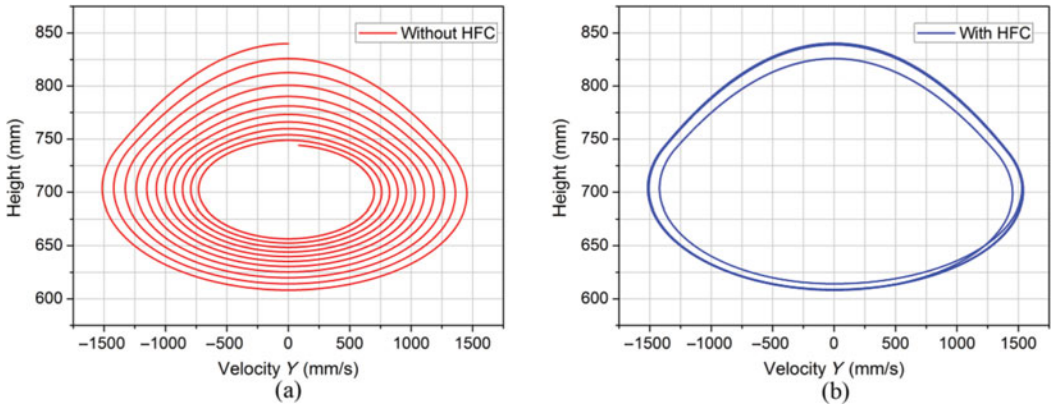

Fig. 9. (Colour online) Phase portraits for the inplace vertical jumping with different control strategies. (a) Control without HFC strategy. (b) Control with HFC strategy.

stable horizontal velocities are set to zero. The expected height of the apex is 840 mm. This experiment focuses itself on the effectiveness verification of dynamic energy compensation of HFC strategy.

We conducted simulation experiments with and without HFC control strategy in application for comparison. As for the model without HFC control strategy in use, the vertical height of the apex in flight phase keep decreasing in every cycle due to spring damping and energy dissipation of contact. While for the model employing HFC control strategy, continuous vertical jumping can be achieved, with the apex height returning to expected value within two cycles. Figure 9 shows phase portraits of these two simulations in comparison, with the horizontal axis showing vertical velocity of the body and the vertical axis presenting its COM height. We can see in the figure that for the system with no HFC control strategy, the state of the model varies with every cycle and its locomotion is an open loop periodical locomotion that cannot converge or keep stable (Fig. 9(a)). On the contrary, locomotion of the system with HFC control strategy converges quickly, forming a closed loop, and realizes the stable control of the SLIP model (Fig. 9(b)). It is clear that the solution converges to a limit cycle.

4.3. Running on a flat terrain

We additionally set initial horizontal velocity of the model to 2.8 m/s to conduct a running simulation experiment on a flat terrain. In this experiment, we have to take into consideration not only the dynamic compensation of the system energy but also the verification of the regulation control of the model contact angle in every cycle. The initial condition remains unchanged, with the control target to be a height of periodical apex of 840 mm and a forward speed of 2.8 m/s. The complexity of the real-time control increases due to the coupling of model's horizontal velocity and the system's energy. The motion sequence diagram of this experiment is shown in Fig. 10.

The simulation results are shown in Fig. 11. The height of the model will decrease after its first contact with the ground, since the default compensation energy of the first cycle is zero. But from the second ground contact, the system will recover its energy quickly and realize periodical jumping (Fig. 11(a)). From the curves of body COM trajectory and horizontal velocity, we can find that the apex height fluctuates in every cycle, but the fluctuation remains little. This agrees with the fluctuation of the body COM and the forward speed of the real dog. Figure 11(b) is the phase portrait of this experiment. We find that except for the relative large variation of return map in the first contact due to lack of compensational energy, this map in the following cycles returns basically to closed curves, which means the stable periodical motion of the system is achieved. As shown in the Figs. 11(c) and (d), the apex height error and the horizontal velocity error are calculated. Relative error quickly converges to a value within 1%, which means the system has been controlled at the target state, thereby achieving the desired periodical motion.

4.4. Running on a sunken terrain

Existing strategies are mostly concerned with the control effects of the model on a flat terrain, paying little attention to the locomotion on an uneven terrain with damping in consideration. We made a trial to apply our HFC control strategy to a simulation experiment of the model on an uneven terrain,

https://doi.org/10.1017/S0263574713001239 Published online by Cambridge University Press

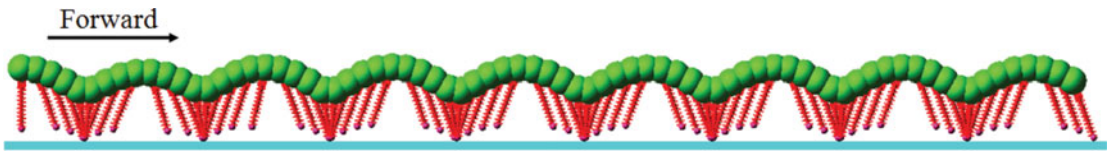

Fig. 10. (Colour online) Motion sequence diagram for running on a flat terrain (desired running speed: 2.8 m/s).

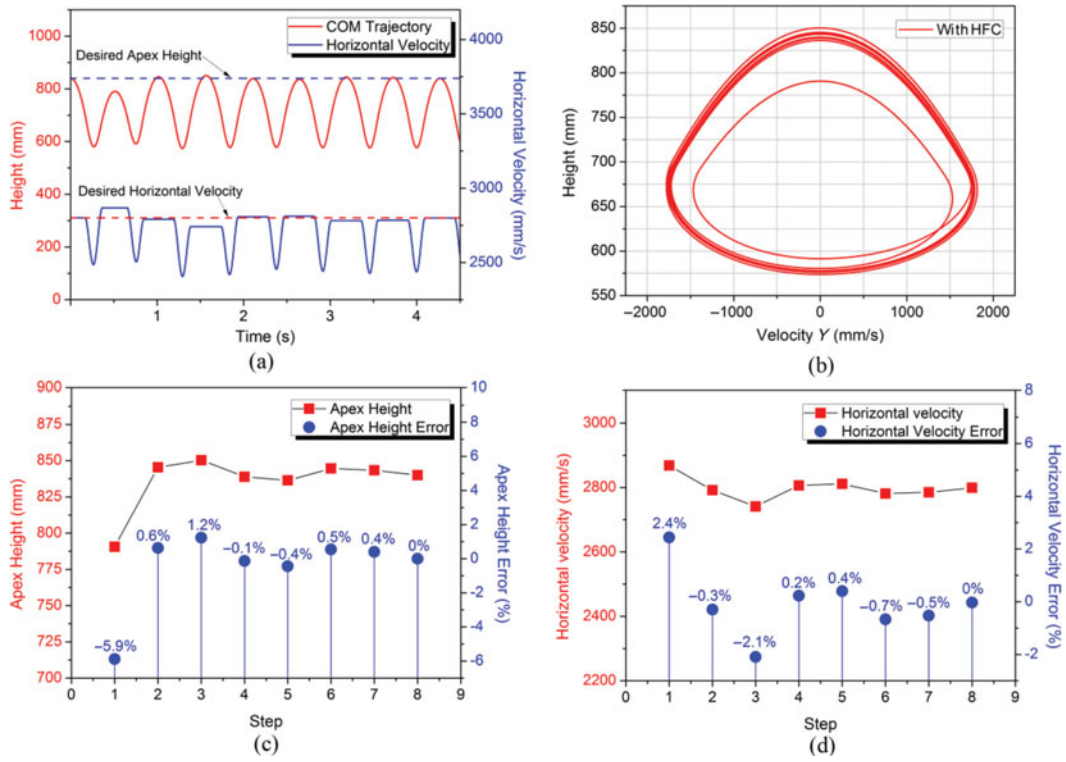

Fig. 11. (Colour online) Simulation results for running on a flat terrain. (a) COM trajectory and horizontal velocity. The desired apex height, $y_{\text{des}}^{\text{APEX}} = 840\,\text{mm}$, and the desired horizontal velocity, $\dot{x}_{\text{des}} = 2800\,\text{mm/s}$. (b) Phase plane trajectory. (c) Apex height error. (d) Horizontal velocity error.

since this strategy employing hybrid feedback according to the previous state has certain robustness and requires no knowledge of terrain.

First, we conduct a simulation of the model on a sunken terrain. Initial condition is set similar to the previous one, with the initial apex height and the forward speed set at 840 mm and 2.8 m/s respectively, and the expected control target remains a height of periodical apex of 840 mm and a forward speed of 2.8 m/s. The sunken height of the terrain that we establish is 50 mm. The system is supposed to keep its stable periodical movement with no information of terrain, and try to achieve the expected control target at the meantime. Figure 12 shows the sequence of movements of the SLIP model running on a sunken terrain.

The simulation results are shown in Fig. 13. Before entering stage 2, the system is able to converge quickly to the expected as running on a flat terrain. When the model steps into stage 2, the energy of the system increases due to the sagging of its body COM. Since HFC control strategy employs hybrid feedback according to a previous state, system state of the first ground contact in stage 2 will go through great fluctuations, but will converge quickly to target one in the following cycles. Process of the model from stage 2 to stage 3 is similar. System state of its first contact phase out of stage 2 varies, but can soon converge to a stable state under the regulation of hybrid feedback (Fig. 13(a)). Figure 13(b) is the phase portrait of current terrain. We can see that although there is fluctuation in the system state, the motion of the system is still able to actively converge to stable state when terrain information is unknown, indicating system's adaptability to different terrain types. The apex height error and the horizontal velocity error are calculated in Figs. 13(c) and (d). Relative error quickly

https://doi.org/10.1017/S0263574713001239 Published online by Cambridge University Press

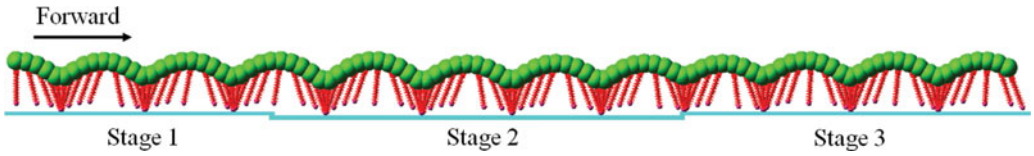

Fig. 12. (Colour online) Motion sequence of running in the sunken terrain (desired running speed: 2.8 m/s).

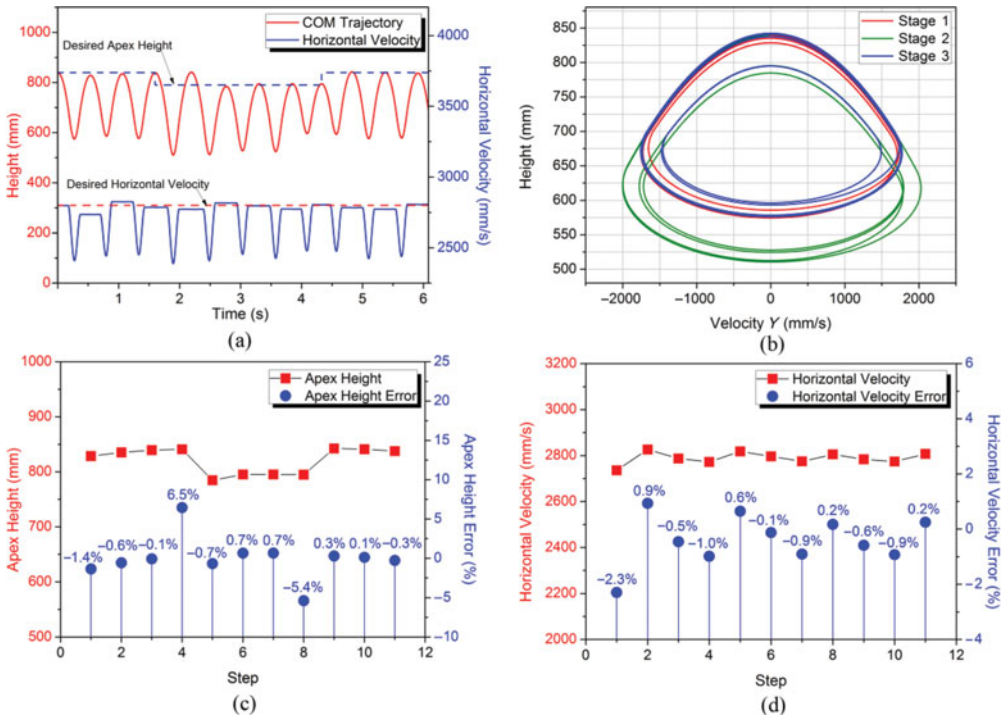

Fig. 13. (Colour online) Simulation results for the SLIP model running in the sunken terrain. (a) COM trajectory and horizontal velocity. The sunken height, $h_{\text{sunken}} = 50$ mm, and the desired horizontal velocity, $\dot{x}_{\text{des}} = 2800$ mm/s. (b) Phase portrait. (c) Apex height error. (d) Horizontal velocity error.

converges to a value in the range of about 1%, which means the system has been controlled at the target state, achieving the desired periodical motion.

4.5. Running down the stairs

We continue to establish another type of uneven terrain, i.e. running down the stairs. The height difference of the stairs is set to 150 mm, 21% of the system length, similar to those in empirical life. The simulation experiment is still conducted on the condition that the terrain is unknown, with initial conditions and control target being the same as in the previous experiment. The initial height is 840 mm and the initial horizontal velocity is 2.8 m/s. The expected control target remains a height of periodical apex of 840 mm and a forward speed of 2.8 m/s. The motion sequence diagram of this experiment is shown in the Fig. 14.

The motion trail of the body COM trajectory of the whole simulation process is presented in Fig. 15(a). It can be seen that the kinetic stability of the system is achieved in the motion process. Every time the terrain changes, compensational energy varies greatly, leading to motion fluctuation. This is because the HFC control strategy employs hybrid feedback, which depends on the previous state. But this variation is controllable and the motion of the system is able to converge in a very short time. Figure 15(b) is the phase portrait of the stairs terrain from which we can find that the return map is able to converge to closed curves, indicating the stable periodical motion achieved by the system. As shown in the Figs. 15(c) and (d), the apex height error and the horizontal velocity error are calculated. Every time, even when terrain condition changes abruptly, introducing great fluctuations

https://doi.org/10.1017/S0263574713001239 Published online by Cambridge University Press

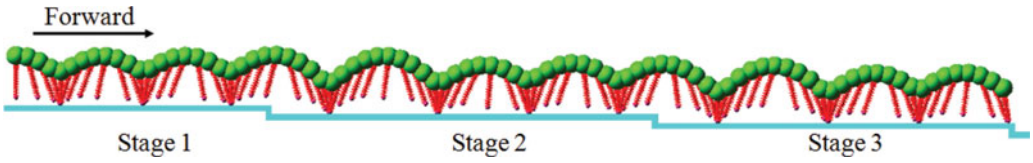

Fig. 14. (Colour online) Motion sequence diagram for running down the stairs (desired running speed: 2.8 m/s).

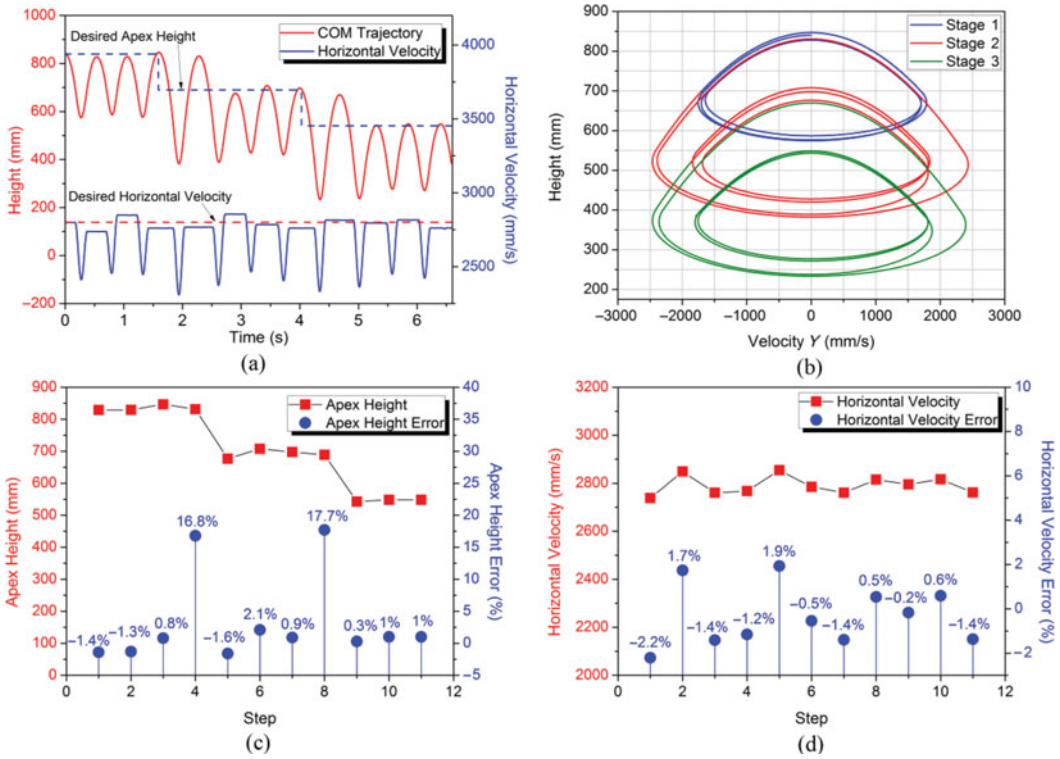

Fig. 15. (Colour online) Simulation results for the SLIP model running down the stairs. (a) COM trajectory and horizontal velocity. The height of the stairs, $h_{\text{stair}} = 150\,\text{mm}$, and the desired horizontal velocity, $\dot{x}_{\text{des}} = 2800\,\text{mm/s}$. (b) Phase portrait. (c) Apex height error. (d) Horizontal velocity error.

into the system, the relative error quickly converges to a value in the range of about 1%. This means the system has been controlled at the target state, achieving the desired periodical motion.

5. Conclusions

A stability control strategy based on HFC is proposed for SLIP running systems considering damping in this paper. The HFC control strategy, including mainly a contact angle controller and a system energy compensator, predicts the values of the contact angle and the compensational energy of the next contact phase by way of comparing the current system state with target one and then realizes the control of the actuators through PD controller and compensational force controller. Because of its employment of hybrid feedback, HFC control strategy has certain robustness and automatic adaptability, and is able to achieve the control target of system's convergence to stability even when the terrain is unknown.

The HFC control strategy reduces the energy fluctuation of the system since it additionally compensates for energy depleted in the current cycle with the amount of depletion in the previous cycle, so a stable periodical motion of the system can be achieved in the shortest time possible. But this requires that the HFC strategy is able to measure the system state of the previous cycle. If terrain condition changes, depletion of contact phase changes as well. Using the compensation value previously calculated will lead to fluctuation in the motion trail of the system, and this is also the

https://doi.org/10.1017/S0263574713001239 Published online by Cambridge University Press

reason for the response lag of the system employing HFC control strategy. Considering fluctuation of the system's motion trail to certain degree is not only acceptable but also inevitable, the HFC strategy can get the system state to converge in the shortest time possible to target one, achieving the periodical stability control of the SLIP system.

To further improve our HFC control strategy, special strategies are applied to the system at the boundary where terrain changes are under development, and an experimental prototype of the SLIP running system with the same driving and sensing system as in simulation is in the process of design and manufacturing. In the following work, we hope to perfect and optimize our HFC control algorithms, and apply these to real robotic systems to verify its control effects.

Acknowledgments

This work is supported by the Science Fund for Creative Research Groups of the National Natural Science Foundation of China under grant number 51121002, the National Natural Science Foundation of China under grant number 61175097, and the 863 Hi-tech R&D Program of China under grant number 2011AA040701.

References

1. M. LaBarbera, "Why the wheels won't go," *Am. Nat.* **121**, 395–408 (1983).
2. C. T. Farley, R. Blickhan, J. Saito and C. R. Taylor, "Hopping frequency in humans: A test of how springs set stride frequency in bouncing gaits," *J. Appl. Physiol.* **71**, 2127–2132 (1991).
3. C. T. Farley and D. C. Morgenroth, "Leg stiffness primarily depends on ankle stiffness during human hopping," *J. Biomech.* **32**, 267–273(1999).
4. K. P. Granata, D. A. Padua and S. E. Wilson, "Gender differences in active musculoskeletal stiffness. Part II. Quantification of leg stiffness during functional hopping tasks," *J. Electromyogr. Kinesiol.* **12**, 127–135 (2002).
5. H. Hobara, K. Kanosue and S. Suzuki, "Changes in muscle activity with increase in leg stiffness during hopping," *Neurosci. Lett.* **418**, 55–59 (2007).
6. R. J. Full, "Mechanics and Energetics of Terrestrial Locomotion: From Bipeds to Polypeds," **In**: *Energy Transformation in Cells and Animals* (W. Wieser and E. Gnaiger, eds.) (Georg Thieme Verlag Press, Stuttgart, Germany, 1989) pp.175–182.
7. R. Alexander, "Three uses for springs in legged locomotion," *Int. J. Robot. Res*. **9**, 53–61 (1990).
8. R. Alexander and A. S. Jayes, "Vertical movements in walking and running," *J. Zool*. **185**, 27–40 (1978).
9. R. J. Full and D. E. Koditschek, "Templates and anchors: Neuromechanical hypotheses of legged locomotion on land," *J. Exp. Biol*. **202**, 3325–3332 (1999).
10. J. G. D. Karssen and M. Wisse, "Running with improved disturbance rejection by using non-linear leg springs," *Int. J. Robot. Res*. **30**, 1585–1595 (2011).
11. R. Blickhan and R. J. Full, "Similarity in multilegged locomotion: Bouncing like a monopode," *J. Comp. Physiol. A-Sens. Neural Behav. Physiol.* **173**, 509–517 (1993).
12. P. Holmes, R. J. Full, D. Koditschek and J. Guckenheimer, "The dynamics of legged locomotion: Models, analyses, and challenges," *SIAM Rev*. **48**, 207–304 (2006).
13. U. Saranli, W. J. Schwind and D. E. Koditschek, "Toward the Control of a Multi-Jointed, Monoped Runner," *Proceedings of IEEE International Conference on Robotics and Automation, 1998 (ICRA '98)*, Leuven, Belgium (May 1998) pp. 2676–2682.
14. R. Blickhan, "The spring-mass model for running and hopping," *J. Biomech*. **22**, 1217–1227 (1989).
15. W. J. Schwind and D. E. Koditschek, "Approximating the stance map of a 2-DOF monoped runner," *J. Nonlinear Sci*. **10**, 533–568 (2000).
16. M. H. Raibert, *Legged Robots that Balance* (MIT Press, Cambridge, MA, 1986).
17. P. Gregorio, M. Ahmadi and M. Buehler, "Design, control, and energetics of an electrically actuated legged robot," *IEEE Trans. Syst. Man Cybern. B-Cybern*. **27**, 626–634 (1997).
18. J. W. Hurst, J. E. Chestnutt and A. A. Rizzi, "Design and Philosophy of the Bimasc, a Highly Dynamic Biped," *Proceedings of IEEE International Conference on Robotics and Automation, 2007 (ICRA 2007)*, Roma, Italy (Apr. 2007) pp. 1863–1868.
19. G. Zeglin, "The Bow Leg Hopping Robot," *Proceedings of IEEE International Conference on Robotics and Automation, 1998 (ICRA'98)*, Leuven, Belgium (May 1998), pp. 781–786.
20. M. Ahmadi and M. Buehler, "The ARL Monopod II Running Robot: Control and Energetics," *Proceedings of IEEE International Conference on Robotics and Automation, 1999 (ICRA '99)*, Detroit, Michigan (May. 1999) pp. 1689–1694.
21. N. Cherouvim and E. Papadopoulos, "Energy saving passive-dynamic gait for a one-legged hopping robot," *Robotica* **24**, 491–498 (2006).
22. R. M. Ghigliazza, R. Altendorfer, P. Holmes and D. E. Koditschek, "A simply stabilized running model," *SIAM J. Appl. Dyn. Syst.* **2**, 187–218 (2003).

https://doi.org/10.1017/S0263574713001239 Published online by Cambridge University Press

23. P. Holmes, "Poincaré, celestial mechanics, dynamical-systems theory and chaos," *Phys. Rep*. **193**, 137–163 (1990).
24. H. Geyer, A. Seyfarth and R. Blickhan, "Spring-mass running: Simple approximate solution and application to gait stability," *J. Theor. Biol*. **232**, 315–328 (2005).
25. U. Saranli, Ö. Arslan, M. M. Ankaralıand Ö. Morgül, "Approximate analytic solutions to non-symmetric stance trajectories of the passive spring-loaded inverted pendulum with damping," *Nonlinear Dyn*. **62**, 729–742 (2010).
26. Y. Haitao, L. Mantian and C. Hegao, "Approximating the Stance Map of the SLIP Runner Based on Perturbation Approach," *Proceedings of IEEE International Conference on Robotics and Automation, 2012 (ICRA 2012)*, St. Paul, MN (May 2012) pp. 4197–4203.
27. S. G. Carver, "Control of a Spring-Mass Hopper," *Ph.D. thesis*, Cornell University, Ithaca, 2003.
28. A. Seyfarth, H. Geyer and H. Herr, "Swing-leg retraction: A simple control model for stable running," *J. Exp. Biol*. **206**, 2547–2555 (2003).
29. Ö. Arslan and U. Saranli, "Reactive planning and control of planar spring–mass running on rough terrain," *IEEE Trans. Robot*. **28**, 567–579 (2012).
30. J. Schmitt and J. Clark, "Modeling posture-dependent leg actuation in sagittal plane locomotion," *Bioinspir. Biomim*. **4**, 046005 (2009).
31. M. Ahmadi and M. Buehler, "Controlled passive dynamic running experiments with the ARL-monopod II," *IEEE Trans. Robot*. **22**, 974–986 (2006).
32. J. K. Hodgins and M. N. Raibert, "Adjusting step length for rough terrain locomotion," *IEEE Trans. Robot. Autom*. **7**, 289–298 (1991).
33. S. H. Hyon and T. Emura, "Energy-preserving control of a passive one-legged running robot," *Adv. Robot.* **18**, 357–381 (2004).
34. H. M. Herr, G. T. Huang, and T. A. McMahon, "A model of scale effects in mammalian quadrupedal running," *J. Exp. Biol*. **205**, 959–967 (2002).
35. C. T. Farley, J. Glasheen and T. A. McMahon, "Running and springs: Speed and animal size," *J. Exp. Biol*. **185**, 71–86 (1993).

https://doi.org/10.1017/S0263574713001239 Published online by Cambridge University Press